

Edge Profile Investigations
Close to the Density Limit of Various Plasma Regimes
in ASDEX Upgrade

V Mertens, H S Bosch, M Kaufmann, M Maraschek, J Neuhauser, H Salzmann,
 J Schweinzer, W Suttrop, ASDEX Upgrade Team

Max-Planck-Institut für Plasmaphysik, EURATOM Association,
 85748 Garching, Fed. Rep. of Germany

Introduction :

The highest achievable density in a tokamak is restricted by an upper boundary called the density limit (DL). In the Ohmic- and L-mode the discharges disrupt when their densities reach this limit. In the H-mode, however, the limit is characterized by a smooth back-transition into the L-mode. Empirically, the density limit is quite successfully described even on machines of different sizes by the Greenwald limit $\bar{n}_e^{GW} = \kappa < j >$ (κ is the plasma elongation and $< j >$ the area averaged plasma current density) [1]. It is originally developed for L-mode discharges with only intrinsic impurities without additional impurity injection. A pronounced feature is its heating power P_{heat} independency. Since the ITER concept aspires an operation density slightly above this limit ($\approx 1.3 \bar{n}_e^{GW}$), one needs reliable scenarios to overcome it without deterioration of the energy confinement time. The H-mode is, therefore, the preferred operation mode. Additionally, the divertor has to be protected against thermic overload as can be caused e.g. by strong ELMs. One possibility is here the addition of impurities which radiate in the edge and remove the power poloidally uniformly as much as possible. Moreover, this method aids the development of divertor detachment. Since both the H- and L-mode density limit is commonly believed to be an edge physics effect, we focus our studies on the boundary. The L-mode density limit is quite well understood as a thermal instability limit (Marfe) and increases moderately with heating power [2]. The physics of the H-mode density limit, which is found to be nearly independent of heating power [2], is on the other hand still not completely unraveled. One explanation recently proposed by FW Perkins [3] connects it with the reach of the ballooning limit, i.e. critical pressure gradients, in the edge. Another attempt is discussed by K Borrass [4] who correlates the limit in both the L- and H-mode with the achievement of full divertor detachment.

This paper deals mainly with the comparison of edge parameter characteristics of conventional gas-puff refuelled H- and L-mode discharges with and without auxiliary impurity seeding. Especially, the density and pressure behaviour will be discussed.

Discharge Parameters and Diagnostics :

Our investigations concentrate on lower single null discharges ($R = 1.65$ m, $a = 0.5$ m, $\kappa \sim 1.6$) in deuterium with plasma currents of 0.8 MA (low \bar{Z}_{eff}) and 1.0 MA (high \bar{Z}_{eff}) applying up to 10 MW NBI heating power. The corresponding safety factors q_{95} vary between 3 and 4. The line averaged electron density \bar{n}_e ranges between $0.8 \cdot 10^{20} m^{-3}$ and $1.2 \cdot 10^{20} m^{-3}$. Highly radiative mantle discharges are performed by injecting mostly Neon gas into the main chamber.

The edge densities and temperatures mainly presented are measured by a Li-beam diagnostics, measuring the local density slightly below the outside midplane and the

Thomson scattering diagnostics measuring n_e and T_e vertically in the outer lower plasma zone.

Experimental Observations :

The H-mode is generally accessible when the power flowing across the separatrix into the boundary $P_{sep} = P_{heat} - P_{rad}^{bulk}$ exceeds a certain limit depending on density and toroidal magnetic field $P_{sep}^{L \rightarrow H} = c \cdot \bar{n}_e B_t$ where the constant c depends mainly on ion species and ion ∇B drift direction [5]. Closely above the threshold the H-mode is characterized by high frequency type-III ELM's ($\partial \nu_{ELM} / \partial P_{sep} < 0$). Deeper in the H-mode the ELM activity changes to low frequency type-I ELMs ($\partial \nu_{ELM} / \partial P_{sep} > 0$) [6].

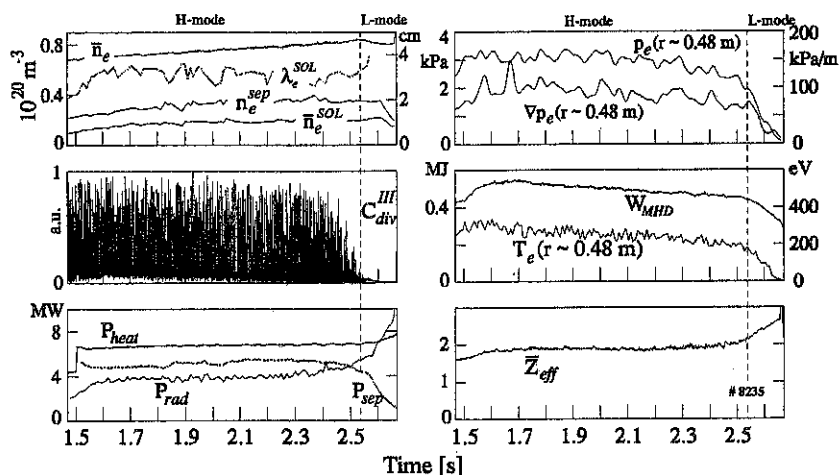


Figure 1: This is an example of a discharge which is successively driven by strong deuterium puffing into H- and L-mode density limit. The vertical dashed lines indicate the H→L-mode back-transition, i.e. the non-disruptive H-mode density limit.

We start with a typical example to reach the density limit in both the H- and L-mode via intense deuterium puffing (see Fig. 1). Since the heating power is well above the threshold the first phase exhibits type-I ELMs. In parallel, strong gas-puffing leads to a smooth increase of \bar{n}_e . The attached divertor regime at low and medium densities alters to detached phases in between ELM's as seen by the drop in the baseline of the C_{div}^{III} signal from 2.3 s. During the ELM's, however, the divertor still reattaches. From about 2.48 s the ELM's exhibit type-III character and the related power flux to the divertor is strongly suppressed. When the power into the edge or the edge temperature falls below a certain value, which coincides with detachment also during type-III ELMs, the discharge falls back into the L-mode (here at ≈ 2.54 s). The correlated densities are associated with the H-mode density limit [2]. The fraction of totally radiated power to heating power varies between 60-70 % and \bar{Z}_{eff} remains below about 2. After the transition in the L-mode the divertor reattaches sometimes depending on the edge parameters. If the endeavours

to increase \bar{n}_e continue, an X-point Marfe develops, grows into the bulk plasma and the discharge disrupts (L-mode density limit) [2]. Applying additional impurity injection, this H/L-mode—disruption sequence is qualitatively very similar, but \bar{Z}_{eff} and radiation fraction is significantly higher with 3-4 and 80-100 %, respectively, and the density profiles are much steeper. The electron temperature profiles, however, are quite insensitive to the regime and depend mainly only on the safety factor.

Focussing on the edge and mostly on the low \bar{Z}_{eff} cases, the local separatrix densities n_e^{sep} are found to rise stronger than the line averaged densities up to the phase where the divertor starts to detach. At the H- and L-mode DL the separatrix density behaves like $n_e^{sep} \propto \bar{n}_e^2$ reflecting the strong broadening of the density profile towards high densities. In parallel, the density decay length λ_e^{SOL} and the line averaged density in the scrape-off layer (SOL) \bar{n}_e^{SOL} increase in the early \bar{n}_e ramp, but saturate close to the H→L-mode back-transition. This saturation effect is clearly seen if one studies \bar{n}_e^{SOL} and λ_e^{SOL} as function of the neutral particle flux densities. Separatrix densities and \bar{n}_e^{SOL} and λ_e^{SOL} of both H- and L-mode show a common linear relationship (see Fig. 2). Typical SOL density decay length are 3-5 cm. Impurity seeded discharges exhibit in the bulk as well as in the SOL (see Fig. 2 b) noticeably more peaked profile shapes. Furthermore, the electron pressure and its gradients ∇p_e increase with P_{heat} , respectively P_{sep} . The gradients close to the edge in type-I ELM phases are found to be nearly constant, $\nabla p_e(0.46m \lesssim r \lesssim 0.50m) \approx const$. At higher density in type-III ELM phases the pressure as well as ∇p_e is clearly reduced and the pressure profiles tend to flatten towards the separatrix $\nabla p_e(r \sim 0.49m) < \nabla p_e(r \sim 0.47m)$, see Fig. 3. Further edge data not restricted to density limit discharges are presented at this conference by W Suttrop [7] and J Schweinzer [8].

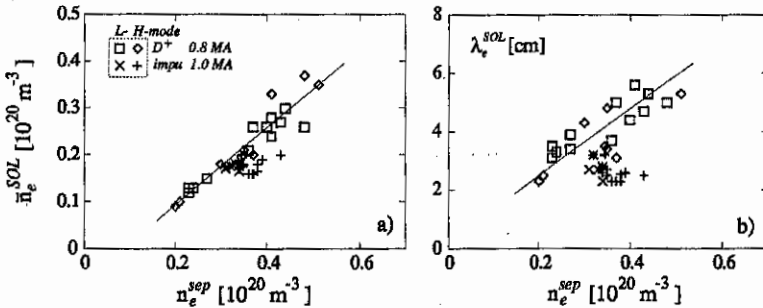


Figure 2: Relation between the separatrix density and the SOL density and decay length at the density limit in different regimes.

There exists another small operational window to reach line averaged densities in the vicinity of the Greenwald limit without external gas-puffing. Slightly above the L→H-threshold at low power fluxes the type-I ELM frequency can be so small that the good H-mode confinement leads to an increase of \bar{n}_e up to the Greenwald limit. In our case frequencies below 100 Hz are necessary. Owing to the missing gas-puff and the correlated low recycling level the confinement is despite high \bar{n}_e not degraded. The achieved \bar{n}_e are even

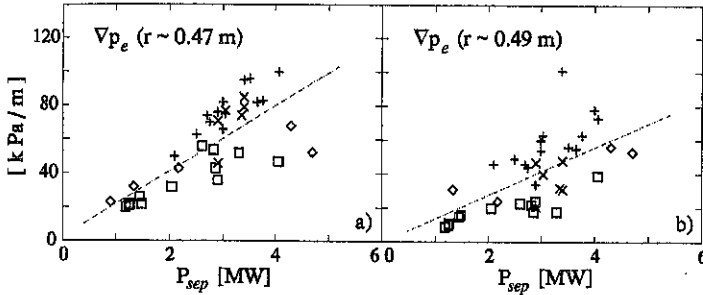


Figure 3: Measured electron pressure gradients in the edge at the density limit in different regimes. The critical gradient for ballooning modes is ≈ 110 kPa/m and ≈ 170 kPa/m for 0.8 MA and 1 MA discharges, respectively.

slightly higher than those produced with strong deuterium puffing. Edge densities and detachment behaviour are, however, clearly representative for low recycling discharges.

Summary :

In ASDEX Upgrade absolute densities in the range of the ITER operation point have been established with pure gas-puffing. In the H-mode the density limit is preceded by divertor detachment in between type-I ELMs and successively a transition to type-III ELM phase with clear detachment. The edge densities and related scale lengths in both H- and L-mode show common behaviour and saturation with developing detachment. The saturation can partly be attributed to the reduction of the penetration depth of neutral particles in the SOL [9]. The pressure gradients are reduced during the approach to the density limit and do clearly not reach the critical pressure gradients for ballooning modes. Additionally, the measured pressure gradients do not seem to scale like $\nabla p_{crit} \propto I_p^2$ as the ballooning mode scaling suggests. The H-mode confinement is, in addition, noticeably reduced close to the H-mode density limit [2].

It is improbable that the operational window connected with low ELM frequencies for achievement of high bulk densities can be used in ITER, since it is very restricted in heating power and the divertor heat load is not mitigated by detachment. In general, the edge data show a stronger correlation of the DL with divertor detachment than with the reach of critical pressure gradients.

References :

- [1] M Greenwald et al, Nuclear Fusion **28**, 1988, 2199
- [2] V Mertens et al, IAEA, 1996, Montreal, IAEA-F1-CN-64/A4-4
- [3] FW Perkins et al, IAEA, 1996, Montreal, IAEA-CN-64/FP-24
- [4] K Borrass et al, Nucl. Fus., **37**, 523 (1997)
- [5] F Ryter et al, Physica Scripta, **51**, 1995, 643
- [6] H. Zohm, Plasma Phys. Control. Fusion **38**, 105 (1996)
- [7] W Suttrop et al, this conference
- [8] J Schweinzer et al, this conference
- [9] J Stober et al, Controlled Fusion and Plasma Physics (Proc. 23rd Europ. Conf. Kiev 1996) **20C** III 1023